Warren-Smith, Stephen; Ebendorff-Heidepriem, Heike; Foo, Tze Cheung; Moore, Roger Charles; Davis, Claire; Monro, Tanya Mary.
Exposed-core microstructured optical fibers for real-time fluorescence sensing, *Optics Express*, 2009; 17(21):18533-18542.

Exposed-core microstructured optical fibers for real-time fluorescence sensing

Stephen C. Warren-Smith[1,*], Heike Ebendorff-Heidepriem[1], Tze Cheung Foo[1], Roger Moore[1], Claire Davis[2], and Tanya M. Monro[1]

[1]*Centre of Expertise in Photonics, Institute for Photonics & Advanced Sensing, The University of Adelaide, Adelaide, Australia*

[2]*Defence Science and Technology Organisation, Fishermans Bend, Victoria, Australia.*

**stephen.warrensmith@adelaide.edu.au*

Abstract: New methods for fabricating glass exposed-core microstructured optical fiber are demonstrated. The fiber designs consist of an optical fiber with a suspended micron-scale core that is partially exposed to the external environment, which is particularly useful for sensing. These fibers allow for strong evanescent field interactions with the surrounding media due to the small core size, while also providing the potential for real-time and distributed measurements. The experimental performance of an exposed-core fiber is compared to an equivalent microstructured fiber with an enclosed (protected) core in terms of their performance as evanescent field sensors. We demonstrate that the exposed-core fiber can provide a significantly improved measurement response time.

OCIS codes: (060.2370) Fiber optics sensors; (060.4005) microstructured fibers; (300.2530) fluorescence, laser-induced.

References and links

1. S. V. Afshar, Y. Ruan, S. C. Warren-Smith, and T. M. Monro, "Enhanced fluorescence sensing using microstructured optical fibers: a comparison of forward and backward collection modes," Opt. Lett. **33**(13), 1473–1475 (2008).
2. S. C. Warren-Smith, S. V. Afshar, and T. M. Monro, "Theoretical study of liquid-immersed exposed-core microstructured optical fibers for sensing," Opt. Express **16**(12), 9034–9045 (2008).
3. Y. Zhu, H. Du, and R. Bise, "Design of solid-core microstructured optical fiber with steering-wheel air cladding for optimal evanescent-field sensing," Opt. Express **14**(8), 3541–3546 (2006).
4. Y. Zhu, R. T. Bise, J. Kanka, P. Peterka, and H. Du, "Fabrication and characterization of solid-core photonic crystal fiber with steering-wheel air-cladding for strong evanescent field overlap," Opt. Commun. **281**(1), 55–60 (2008).
5. H. Ebendorff-Heidepriem, S. C. Warren-Smith, and T. M. Monro, "Suspended nanowires: fabrication, design and characterization of fibers with nanoscale cores," Opt. Express **17**(4), 2646–2657 (2009).
6. Y. Ruan, T. C. Foo, S. C. Warren-Smith, P. Hoffmann, R. C. Moore, H. Ebendorff-Heidepriem, and T. M. Monro, "Antibody immobilization within glass microstructured fibers: a route to sensitive and selective biosensors," Opt. Express **16**(22), 18514–18523 (2008).
7. S. Afshar, S. C. Warren-Smith, and T. M. Monro, "Enhancement of fluorescence-based sensing using microstructured optical fibres," Opt. Express **15**(26), 17891–17901 (2007).
8. J. B. Jensen, P. E. Hoiby, G. Emiliyanov, O. Bang, L. H. Pedersen, and A. Bjarklev, "Selective detection of antibodies in microstructured polymer optical fibers," Opt. Express **13**(15), 5883–5889 (2005).
9. J. B. Jensen, L. H. Pedersen, P. E. Hoiby, L. B. Nielsen, T. P. Hansen, J. R. Folkenberg, J. Riishede, D. Noordegraaf, K. Nielsen, A. Carlsen, and A. Bjarklev, "Photonic crystal fiber based evanescent-wave sensor for detection of biomolecules in aqueous solutions," Opt. Lett. **29**(17), 1974–1976 (2004).
10. Y. L. Hoo, W. Jin, C. Shi, H. L. Ho, D. N. Wang, and S. C. Ruan, "Design and modeling of a photonic crystal fiber gas sensor," Appl. Opt. **42**(18), 3509–3515 (2003).
11. H. Lehmann, J. Kobelke, K. Schuster, A. Schwuchow, R. Willsch, and H. Bartelt, "Microstructured index-guiding fibers with large cladding holes for evanescent field chemical sensing," Proc. SPIE **7004**, 70042R (2008).
12. C. M. B. Cordeiro, E. M.D. Santos, C. H. Brito Cruz, C. J. S. de Matos, and D. S. Ferreiira, "Lateral access to the holes of photonic crystal fibers - selective filling and sensing applications," Opt. Express **14**(18), 8403–8412 (2006).
13. C. M. B. Cordeiro, C. J. S. de Matos, E. M. dos Santos, A. Bozolan, J. S. K. Ong, T. Facincani, G. Chesini, A. R. Vaz, and C. H. Brito Cruz, "Towards practical liquid and gas sensing with photonic crystal fibres: side access to the fibre microstructure and single-mode liquid-core fibre," Meas. Sci. Technol. **18**(10), 3075–3081 (2007).

14. C. Martelli, P. Olivero, J. Canning, N. Groothoff, B. Gibson, and S. Huntington, "Micromachining structured optical fibers using focused ion beam milling," Opt. Lett. **32**(11), 1575–1577 (2007).
15. A. van Brakel, C. Grivas, M. N. Petrovich, and D. J. Richardson, "Micro-channels machined in microstructured optical fibers by femtosecond laser," Opt. Express **15**(14), 8731–8736 (2007).
16. C. J. Hensley, D. H. Broaddus, C. B. Schaffer, and A. L. Gaeta, "Photonic band-gap fiber gas cell fabricated using femtosecond micromachining," Opt. Express **15**(11), 6690–6695 (2007).
17. H. C. Nguyen, B. T. Kuhlmey, E. C. Magi, M. J. Steel, P. Domachuk, C. L. Smith, and B. J. Eggleton, "Tapered photonic crystal fibres: properties, characterisation and applications," Appl. Phys. B **81**(2-3), 377–387 (2005).
18. F. M. Cox, R. Lwin, M. C. J. Large, and C. M. B. Cordeiro, "Opening up optical fibres," Opt. Express **15**(19), 11843–11848 (2007).
19. A. Karagiannis, A. N. Hrymak, and J. Vlachopoulos, "Three-dimensional non-isothermal extrusion flows," Rheol. Acta **28**(2), 121–133 (1989).
20. G. Brambilla, F. Xu, and X. Feng, "Fabrication of optical fibre nanowires and their optical and mechanical characterisation," Electron. Lett. **42**(9), 517–519 (2006).
21. Y. L. Hoo, W. Jin, H. L. Ho, D. N. Wang, and R. S. Windeler, "Evanescent-wave gas sensing using microstructure fiber," Opt. Eng. **41**(1), 8–9 (2002).
22. G. Pickrell, W. Peng, and A. Wang, "Random-hole optical fiber evanescent-wave gas sensing," Opt. Lett. **29**(13), 1476–1478 (2004).
23. T. Ritari, J. Tuominen, H. Ludvigsen, J. C. Petersen, T. Sørensen, T. P. Hansen, and H. R. Simonsen, "Gas sensing using air-guiding photonic bandgap fibers," Opt. Express **12**(17), 4080–4087 (2004).

1. Introduction

Microstructured optical fibers (MOFs) and optical nanowires have the ability to provide a large proportion of the guided optical power either to the external environment or the holes within the MOF. Of particular interest is the jacketed and suspended nano/micro-wire design [1–6] (wagon wheel fiber), as this provides a means for protecting the highly sensitive optical wire, and long lengths can be fabricated by drawing a structured preform. Currently, core diameters have been reduced to values as low as 410nm in lead silicate glass [5]. As this is smaller than the wavelength of light used in most sensing applications, a large percentage of the evanescent field can be used to interact with an analyte, allowing sensing via absorption or fluorescence processes. In addition, it has been shown theoretically that small core diameter fibers, particularly those with a high refractive index substrate material, can efficiently capture fluorescence into the guided modes of the fiber [1, 2, 7]. A broad range of sensing applications exists using this design of sensor due to the ability to functionalize the surface for biological applications [6, 8], as well as other chemical applications. While in principle long interaction lengths can be achieved using MOFs, in practice the difficulty exists that fibers of the type described above can only be filled from one of the distal ends (via capillary forces for liquids [7, 9] or diffusion for gases [10]). Typical filling times include greater than four hours to fill half a meter of fiber with isopropanol (liquid) [7] and 200 minutes to fill 1 m of fiber with acetylene (gas) [10]. While pressure can be used to improve the filling time [9], filling greater than a few meters takes an impractically long time and thus cannot lead to a real-time sensor. Likewise, there is some scope for increasing the size of the holes within the MOF so that filling times are improved [11], but again real-time sensing is not possible. Note that if the analyte changes during the measurement period, emptying and re-filling of the fiber is required. In addition, it is not possible to perform distributed sensing with traditional MOFs due to the requirement to fill from the distal ends. These issues can, in principle, be solved by exposing the core along the length of MOFs.

The exposed-core fiber was first proposed in 2003 by Hoo et al [10] and fabrication has since been demonstrated by the use of a fusion splicer and air pressure to blow holes within an MOF [12], use of a focused ion beam [13, 14], and femtosecond laser micromachining [15, 16]. Also, tapering of MOFs can allow access to the guided optical field [17]. However, these methods generally result in short exposed regions, such as the order of tens of microns. Cox *et al.* have shown that long lengths of exposed-core polymer fiber can be fabricated by creating an opening at the preform stage of the fiber fabrication, such as by drilling holes into the cladding of a polymer MOF preform [18]. In this paper we present two new methods for fabricating exposed-core fiber, and demonstrate these methods using lead-silicate glass fibers. The first method involves etching the drawn fiber to expose the core; while the second involves directly drawing the exposed-core fiber. We then demonstrate that the fabricated

fibers can successfully measure fluorescence with a response time substantially quicker than for an equivalent protected-core MOF.

2. Fabrication

Our method of fabrication expands on the method previously developed for fabricating enclosed wagon wheel (WW) fibers via preform extrusion, caning, and drawing of soft glass [5]. Here a lead-silicate glass (Schott glass F2, n ≈1.62) was used. The process is summarized in Fig. 1. First, a WW structured preform and wedged jacket were extruded from stainless steel dies at high temperature and pressure. The WW preform was caned using a fiber drawing tower and inserted into the jacket. The cane-in-jacket preform was then drawn into fiber with an outer diameter of approximately 160μm, with core diameters ranging from 2.0 to 3.0 μm. The advantage of extrusion for this fiber design is significant, as it allows the fabrication of asymmetric structures such as the wedged jacket. However, this proved to be a challenge in practice, due to the tendency of the preform to bend as a result of temperature asymmetries resulting from the use of an asymmetric wedged jacket die. This caused an asymmetry in the viscosity profile and thus bending in the preform during extrusion. In addition, the use of an asymmetric die can cause bending, even in isothermal conditions [19]. Several methods were employed to overcome preform bending. The most successful method was found to be attachment of a stainless steel pole to the wedged jacket at the start of the extrusion to mechanically force it along a straight line.

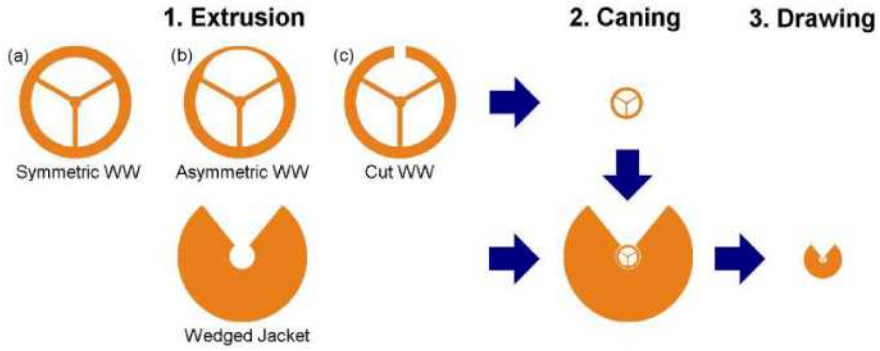

Fig. 1. Schematic diagram of the fabrication process.

As indicated in Fig. 1, several fiber designs were trialed for their suitability in fabricating this type of exposed core fiber. A summary of these trials is included here for clarity in Table 1, where a description of each of the trials follows. Loss measurements from Sec. 3 have also been briefly included.

Table 1. Summary of the exposed-core fiber fabrication trials. Loss values have been included from Sec. 3.

Trial number	WW die	Etching required	Loss before etching (dBm^{-1} at 1000nm)	Loss after etching (dBm^{-1} at 532nm)
1	Symmetric WW	Yes	2.8 ± 0.2	Fiber too damaged
2	Asymmetric WW	Yes	2.1 ± 0.2	54 ± 5
3	Cut WW (standard struts)	No	4.1 ± 0.2	N/A
4	Cut WW (thick struts)	No	2.2 ± 0.3	N/A

Using a symmetric WW preform (Fig. 1(a)), the fiber shown in Fig. 2(a) and (b) was drawn (trial #1) and by using an asymmetric WW preform (Fig. 1(b)) the fiber shown in Fig. 3(a) and (b) was drawn (trial #2). Approximately 100-150m of each fiber type was drawn, each from a single preform. Note that these fibers are not yet fully exposed at the time of drawing due to the presence of a cover layer. This cover layer was used to protect the core during the fiber drawing, and assisted in maintaining the fiber structure by allowing self-pressurization of all three fiber holes. We refer to these fibers as protected-core fibers.

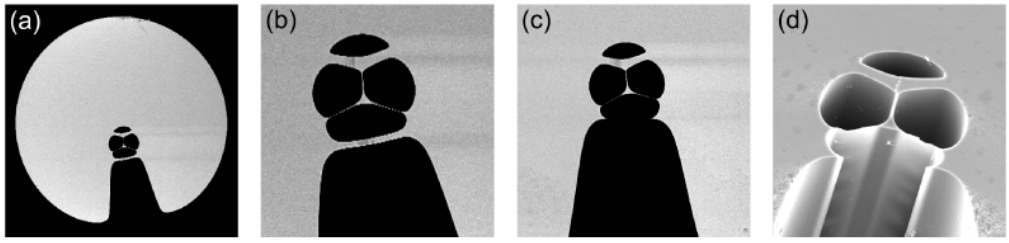

Fig. 2. Trial #1 exposed-core fibers fabricated from a symmetric WW preform, the image sizes are (a) 200μm, (b) 80μm, (c) 80μm, and (d) 40μm. Images (c) and (d) show the fiber after HF etching.

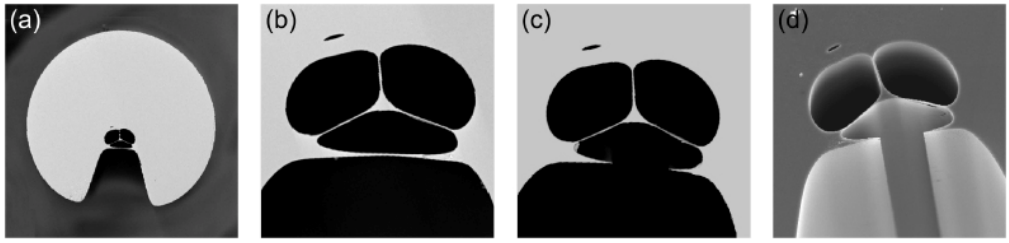

Fig. 3. Trial #2 exposed-core fibers fabricated from an asymmetric WW preform, the image sizes are (a) 200μm, (b) 35μm, (c) 35μm, and (d) 40μm. Images (c) and (d) show the fiber after HF etching.

The cover layer was removed through chemical etching with 0.056±0.001 wt. % hydrofluoric acid (HF). This was experimentally determined to have an etch rate of 30±1 nm/min at the site of the cover layer while 25 cm of a 33 cm length of fiber with both ends sealed was fully immersed in the acid, held vertically, and rotated at 78 rpm. Vertical orientation and rotation of the fiber was found to be necessary in order to produce a consistent etch rate along a reasonable length of the fiber. The required etch time was determined to be 78 mins for the trial #1 fiber (Fig. 2) and 11.3 mins for the trial #2 fiber (Fig. 3). For the fiber produced in trial #1, it was not found to be possible to completely etch through the cover layer along the entire length of fiber without etching through the struts at some point due to the cover layer being considerably larger than the struts. The fiber from trial #2 had a much

improved strut to cover layer ratio (48% compared to 12%), and was thus successfully etched without damaging the struts.

To avoid the requirement for HF etching, we trialed the direct-drawing of exposed-core fibers by cutting a thin slot into the side of a symmetric WW preform as shown in Fig. 1(c). This was then caned and drawn into the fiber shown in Fig. 4 (trial #3). The advantage of this method is that exposed-core fiber is produced straight from the fiber draw stage, which allows significantly longer lengths of exposed-core fiber to be fabricated. However, the fiber core is unprotected during the caning and drawing processes. The struts also become elongated due to surface tension effects, with a final thickness of 70±10 nm, compared with 160±10 nm for the fiber shown in Fig. 3(c). This accounts for an observed increase in fiber fragility for the directly-drawn exposed-core fiber. In particular, the core tended to break during use, even while the cladding remained intact. Also note the ribbed effect along the struts in Fig. 4(d), which indicates stress in the struts. To improve fiber strength, particularly in the region supporting the core, the strut thickness was doubled in the WW preform with the resulting fiber shown in Fig. 5 (trial #4). This fiber was significantly easier to handle, and no breakage of the core during use has yet been observed.

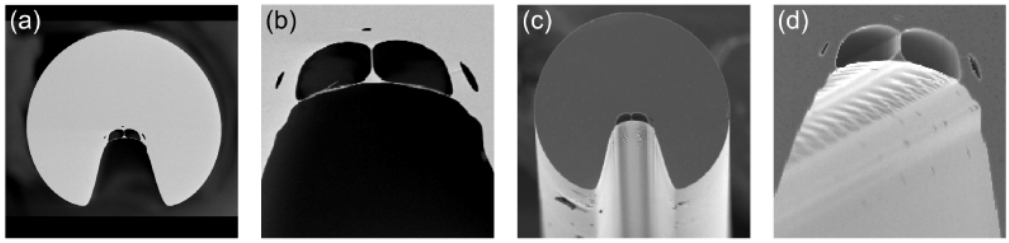

Fig. 4. Trial #3 exposed-core fibers fabricated from a symmetric WW preform with slot and standard strut thickness. The image sizes are (a) 200μm, (b) 50μm, (c) 200μm, and (d) 40μm.

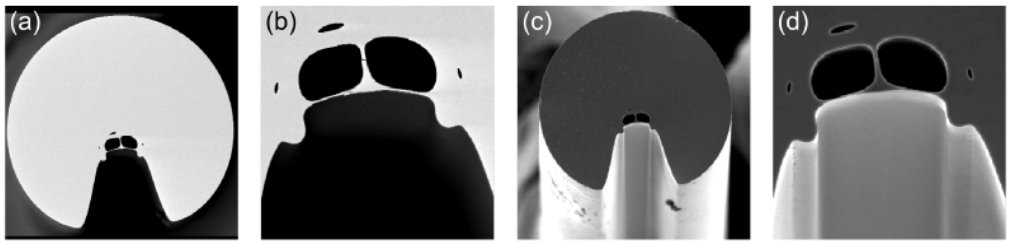

Fig. 5. Trial #4 exposed-core fibers fabricated from a symmetric WW preform with slot and increased strut thickness. The image sizes are (a) 170 μm, (b) 40 μm, (c) 200 μm, and (d) 40 μm.

To the best of our knowledge this is the first demonstration of glass exposed-core microstructured optical fiber produced directly from fiber drawing. The length of fiber produced from a single draw for both trial #3 and #4 was the order of 200 m, which is a significant improvement on previous pointwise methods where reported lengths of the exposed region include 64μm [12] and 20 μm [13].

3. Propagation loss

The propagation loss spectra of trial #1 and #2 fibers before etching, along with trial #3 and #4 fibers, were measured using the standard cutback measurement technique. A supercontinuum white light source (KOHERAS SuperK^{TM} Compact) was collimated and then focused into the fibers using a 2.75 mm focal length lens. The output signal was launched into an optical spectrum analyzer (OSA) using free space coupling after collimation with a 40X microscope objective lens. Both the input and output coupling was maximized at 1000 nm so

that the measurements were repeatable when successive cutbacks were made. The results are shown in Fig. 6.

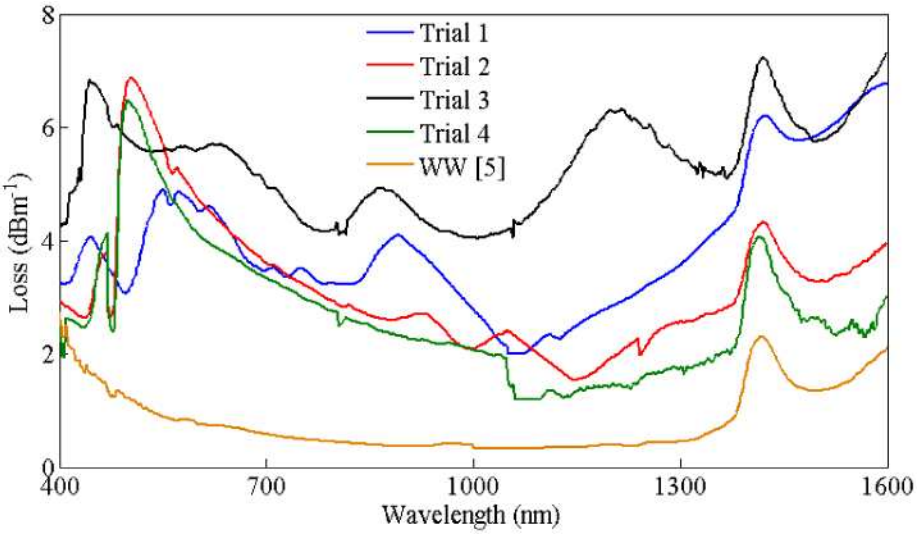

Fig. 6. Measured loss for trial #1 protected-core fiber (blue), trial #2 protected-core fiber (red), trial #3 directly-drawn exposed-core fiber (black), and trial #4 directly-drawn exposed-core fiber (green). The WW preform used to fabricate the trial #4 fiber was ultrasonically cleaned prior to fiber drawing. The loss of an enclosed wagon wheel fiber with a similar core diameter (2.1 μm, compared to 2.0-3.0 μm) has been included for comparison (orange) [5]. The WW preform used to fabricate this fiber was also ultrasonically cleaned.

The results show that the propagation loss of the first directly-drawn exposed-core fiber (trial #3) is approximately 2 dBm^{-1} higher relative to the protected-core fibers (trials #1 and #2). This is likely to be due to surface contamination post-caning and post-drawing, as no cleaning was performed beyond the preform stage. It is also possible that surface cracks may have formed in the time between drawing and measurement as a result of exposure to moisture [20], and this effect would also likely lead to increased long term loss for the fiber. For this reason the exposed-core fibers were stored in a moisture-free environment when not in use. In order to improve the directly-drawn exposed-core fiber loss, the WW preform used to fabricate the trial #4 fiber was ultrasonically cleaned prior to caning. Ultrasonic cleaning of the preform is a standard procedure for WW fiber fabrication [5], but had not been performed on previous exposed-core fiber trials due to concerns over strut fragility. The improvement can be observed by comparing the loss of trial #3 and #4 fiber in Fig. 6, where the average loss across the whole spectrum was reduced by 2.4 dBm^{-1}. However, comparing the loss between the trial #4 fiber and that of a previously reported enclosed wagon wheel fiber (Fig. 6, orange) we see that the exposed-core fiber still has significantly higher loss. The reasons for this excess loss are not yet clear, although it is anticipated that improved preform cleaning and fiber storage conditions will assist in reducing the exposed-core fiber loss.

These measurements were performed on the fiber immediately after drawing, but for trials #1 and #2 the fiber is not exposed at this point as they required chemical etching. Trial #1 fiber could not be etched consistently enough to perform a loss measurement. The loss of trial #2 fiber after HF etching was measured as 54±5 dBm^{-1} at 532 nm, compared to 6±1 dBm^{-1} for the unetched, protected-core fiber. This was measured by comparing the transmission of etched and unetched fiber of the same length (25 cm), which assumes that the coupling is the same for both cases. This high loss was caused by an increase in the surface roughness due to the HF etching, as observed with atomic force microscopy measurements performed on bare fiber (no structure) under identical etching conditions to that of the trial #2 exposed-core fiber (Fig. 7).

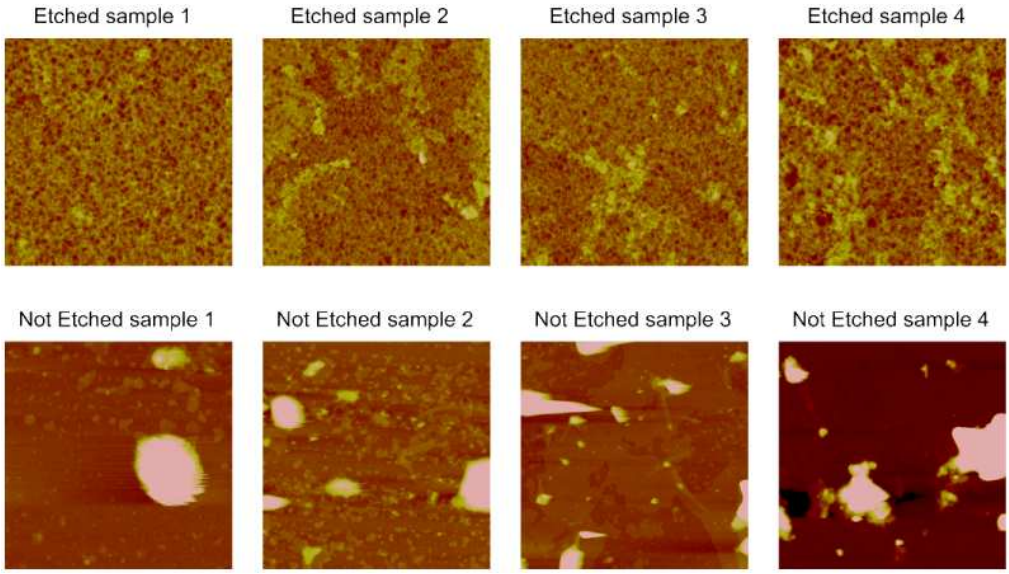

Fig. 7. Atomic force microscopy images of the surface of HF etched bare fiber (upper images) and the surface without etching (lower images). The images sizes are 5 μm x 5 μm and the image height spans 50 nm.

The images in Fig. 7 exhibit considerable differences in the surface before and after etching with HF. The etched surface appears to be considerably rougher, while the non-etched surface is relatively smooth with the exception of large pieces of debris. These large pieces are likely due to surface contamination during storage (1 month), which could not be successfully removed when cleaned with ethanol and water prior to mounting for AFM measurements. These surfaces are not likely to be representative of the fiber surface quality immediately after fabrication, particularly when considering that the exposed-core fiber is partially protected by the wedged jacket. These large pieces of debris are not visible on the etched surface, which suggests they were removed from the surface during the HF etching process. Thus, discounting the large debris pieces, the surface quality of the etched surface is visibly rougher and accounts for the high loss measured for the etched, exposed-core fiber.

Unfortunately, the high level of loss due to HF etching means this method of exposed-core fiber fabrication is not well suited to fabricating lengths of more than tens of centimeters unless the etching process can be improved. In addition, there are practical challenges in accurately etching large lengths of fiber, say, greater than one meter. However, one possibility for distributed sensing is to choose to expose only selected locations along the fiber whilst leaving the majority of the fiber inactive and thus protected. This could prove useful in applications where multi-point sensing is required in a quasi-distributed system or to improve MOF filling times.

4. Fluorescence measurements

In general, evanescent-field microstructured optical fiber sensing has either made use of absorption or fluorescence based techniques. Absorption is commonly used for gas sensing [16, 21–23] while fluorescence tends to be used for biological applications where fluorescent labels are often used [6,8]. One drawback of the MOF sensing method is that the measurement response time is related to the time required to fill the fiber. Here we demonstrate that one useful application of the exposed-core fiber is to reduce the time of filling an MOF, and thus to dramatically improve the response time of the sensor. Here we present experimental results of the response time for fluorescence sensing with exposed-core fibers, and compare these to using enclosed (protected) core fibers.

To measure the response time for the exposed-core fiber the experimental setup shown in Fig. 8(a) was used where 532 nm laser light was focused into directly-drawn exposed-core fiber (trial #4, Fig. 5), and the output was directed through a long pass filter and into a spectrometer. The fiber was placed into an empty bath which was filled with $2x10^{-6}$ M Rhodamine B in water while recording the spectral response over time.

To compare the response time an unetched, enclosed (protected) core fiber was also tested (trial #2 not-etched, Fig. 3(a, b)). For the enclosed (protected) core fiber the test fluorophore was a 91 nM solution of organic quantum dots (QDot800™, Invitrogen) dissolved in hexadecane, which was allowed to fill into the fiber via capillary forces. The experimental setup is shown in Fig. 8(b). The 532 nm excitation light was reflected from a long pass dichroic mirror (R532 T633) and focused into the fiber using a short focal length aspheric lens (f = 2.75 mm) and a nano-positioning stage. The fluorescence signal collected by the fiber was imaged using the same aspheric lens, passed through the dichroic mirror, filtered using a 550 nm long pass filter, measured using a low power photo-detector, and the data logged with a power meter.

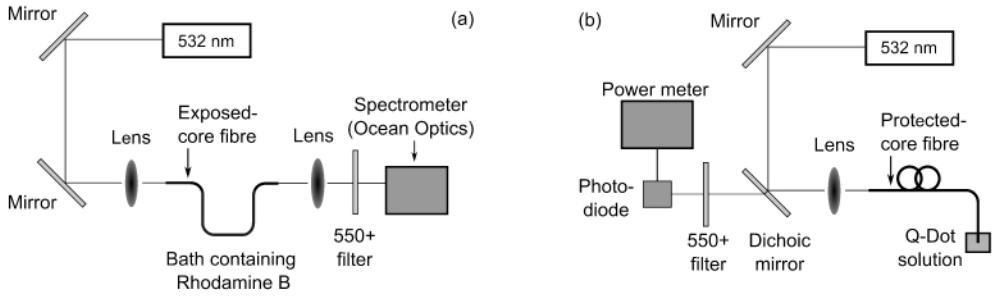

Fig. 8. Experimental setup for measuring the fluorescence sensor time response for (a) exposed-core fiber (trial #4, Fig. 5) and (b) enclosed (protected) core fiber (trial #2 not-etched, Fig. 3 (a, b)).

Note that quantum dots were used for the enclosed (protected) core fiber to avoid the effect of photobleaching, which is significant when small quantities of fluorophore are used [7]. An organic dye was used for the exposed-core fiber due to the large volume of fluorophore required to fill the bath. Also, a spectrometer was used to measure the Rhodamine B fluorescence in order to help differentiate the pump and fluorescence signals, which was not necessary for the quantum dots due to the large separation of excitation and fluorescence wavelengths. The fluorescence sensing time response measurements for the exposed-core fiber are shown in Fig. 9, and for the enclosed (protected) core fiber in Fig. 10.

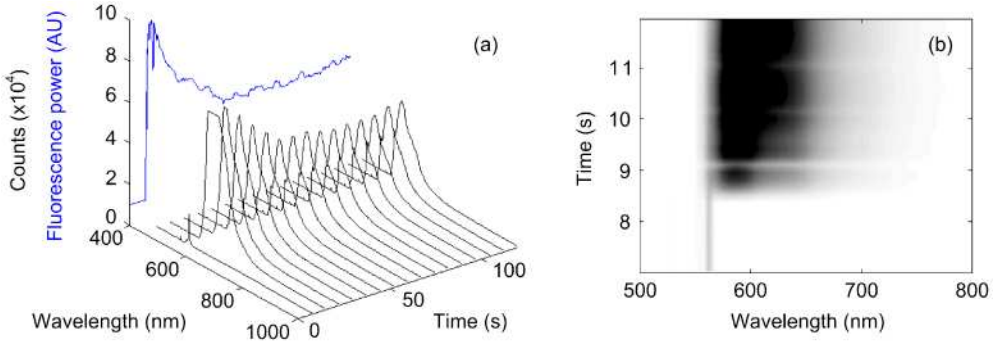

Fig. 9. (a) The spectral signal recorded over time using an exposed-core fiber (trial #4, Fig. 5) as the bath was filled with Rhodamine B. (b) Same as for (a) considering the initial few seconds only.

As expected, a strong fluorescence signal was obtained after filling the bath with Rhodamine B, which then decayed initially due to photobleaching [7], and then reached a stable level. The fluorescence power curve in Fig. 9(a), together with Fig. 9(b), shows that the time taken to reach a strong fluorescence signal is the order of one second for the exposed-core fiber. We now compare this to the results obtained using the enclosed (protected) core fiber, which are shown in Fig. 10.

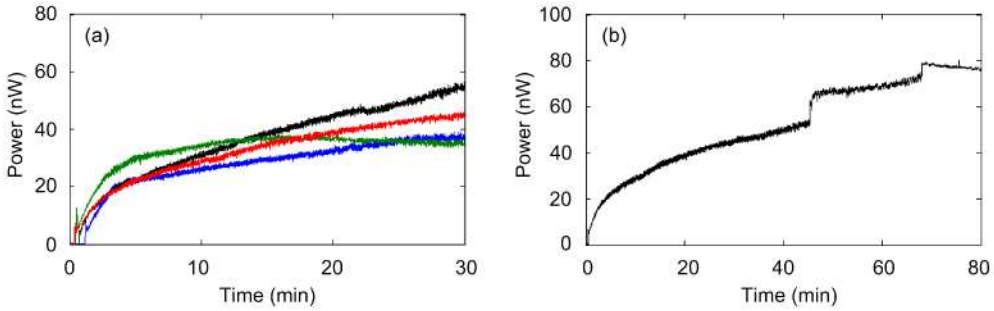

Fig. 10. Fluorescence signal measured for the enclosed (protected) core fibers (trial #2 before etching) over 30 mins (a) and 80 mins (b). Different colors refer to repeats of the same experiment.

The results in Fig. 10 for the enclosed (protected) core fiber show a more gradual increase in fluorescence, which corresponds to the capillary filling time of the fiber. The sharp steps shown in Fig. 10(b) correspond to times when the holes of the fiber became completely filled, and thus the coupling efficiency at the input end of the fiber changes (because the fluid has reached the launch end of the fibre). Comparing the two fiber designs, the exposed-core fiber reached a maximum fluorescence signal after approximately one second, while the enclosed (protected) core fiber required approximately 70 minutes to completely fill and hence reach a maximum signal.

5. Conclusions

Two methods for fabricating glass exposed-core microstructured optical fiber have been demonstrated. In the first method a soft-glass extruded preform was drawn into a fiber and then chemically etched to expose the small and thus highly-sensitive core. This method was demonstrated with two different fiber designs and it was observed that reducing the amount of glass to be etched allowed for the fabrication of consistent lengths of exposed-core fiber. In the second method the wagon wheel preform is cut prior to caning, so that the drawn fiber is exposed without requiring etching. The advantage of the etching method is that the fiber core is protected during the fabrication process, which is reflected in the reasonably low loss immediately after drawing. However, ultrasonic cleaning of the preform before caning can be used to improve the loss of directly-drawn exposed-core fiber. In addition, the surface roughness and resultant optical loss due to hydrofluoric acid etching means that directly drawing exposed-core fiber is, at present, the preferred method for fiber fabrication.

The directly-drawn exposed-core fiber was evaluated for fluorescence-based sensing, in order to determine the measurement response time and compare with enclosed MOF sensors. The exposed-core fiber was placed in a bath that was filled with a fluorophore and the measurements were made in the forwards direction. While ideal for demonstrating the capability of the exposed-core fiber, this type of experimental arrangement does not allow for small volumes of analyte to be measured. The signal response time for the exposed-core fiber was found to be significantly faster than for the enclosed (protected) core fiber. Given the ability to do almost real-time sensing and the possibility for distributed sensing it is anticipated that exposed-core fibers will in the future play an important role to the field of chemical and biological sensing.

Acknowledgments

We acknowledge the support of the Defence Science and Technology Organisation (DSTO), Australia, and in particular the DSTO Corporate Initiative on Smart Materials and Structures for sponsorship of this program of research. We acknowledge the Australian Research Council for funding this project (DP0880436). T. Monro acknowledges the support of an Australian Research Council Federation Fellowship.